A Journal of the Gesellschaft Deutscher Chemiker

Angewandte International Edition GDCh Chemie

www.angewandte.org

Accepted Article

Title: Post-Functionalization of Supramolecular Polymers on Surface and the Chiral Assembly-Induced Enantioselective Reaction

Authors: Deng-Yuan Li, Ya-Cheng Zhu, Shi-Wen Li, Chen-Hui Shu, and Pei Nian Liu

To be cited as: *Angew. Chem. Int. Ed.* 10.1002/anie.202016395

Link to VoR: https://doi.org/10.1002/anie.202016395

WILEY-VCH

10.1002/anie.202016395

RESEARCH ARTICLE

WILEY-VCH

Post-Functionalization of Supramolecular Polymers on Surface and the Chiral Assembly-Induced Enantioselective Reaction

Deng-Yuan Li[+], Ya-Cheng Zhu[+], Shi-Wen Li, Chen-Hui Shu and Pei-Nian Liu*

[*] Dr. D.-Y. Li, Y.-C. Zhu, S.-W. Li, Dr. C.-H. Shu, Prof. Dr. P.-N. Liu
Key Laboratory for Advanced Materials and Feringa Nobel Prize Scientist Joint Research Center, Frontiers Science Center for Materiobiology and Dynamic Chemistry, State Key Laboratory of Chemical Engineering, School of Chemistry and Molecular Engineering, East China University of Science & Technology, 130 Meilong Road, Shanghai, 200237, China
E-mail: liupn@ecust.edu.cn
[+] These authors contributed equally to this work.

Supporting information for this article is given via a link at the end of the document.

Abstract: Although post-functionalization is extensively used to introduce diverse functional groups into supramolecular polymers (SPs) in solution, post–functionalization of SPs on surfaces still remains unexplored. Here we achieved the on-surface post-functionalization of two SPs derived from 5,10,15-tri-(4-pyridyl)-20-bromophenyl porphyrin (Br-TPyP) via cross-coupling reactions on Au(111). The ladder-shaped, Cu-coordinated SPs preformed from Br-TPyP were functionalized through Heck reaction with 4-vinyl-1,1'-biphenyl. In the absence of Cu, Br-TPyP formed chiral SPs as two enantiomers via self-assembly, which were functionalized via divergent cross-coupling reaction with 4-isocyano-1,1'-biphenyl (ICBP). Surprisingly, this reaction was discovered as an enantioselective on-surface reaction induced by the chirality of SPs. Mechanistic analysis and DFT calculations indicated that after debromination of Br-TPyP and the first addition of ICBP, only one attack direction of ICBP to the chiral SP intermediate is permissive in the second addition step due to the steric hindrance, which guaranteed the high enantioselectivity of the reaction.

Introduction

Supramolecular polymers (SPs) are polymeric chains held together by reversible, highly directional non-covalent interactions such as hydrogen bonds and coordination bonds.[1] SPs exhibit traditional characteristics of polymers as well as unique properties such as sensitive response to stimuli, self-repair capacity, and adaptation to the microenvironment.[2] Indeed, functionalized SPs offer mechanical, biological, optical and electronic properties that have driven innovation in various areas.[3] SP monomers can be functionalized before their self-assembly into polymers (pre-functionalization) or afterward (post-functionalization). Pre-functionalization has been used to construct diverse supramolecular architectures as the bottom-up protocol, although every SP needs a specific monomer.[3c,3d] Through post-functionalization,[4-6] one monomer forms a SP as the backbone, which can be functionalized to afford diverse SPs. Since post-functionalization can easily achieve diverse SPs, it has been extensively used in the labeling of biomolecules[5] such as DNAs[5b] and proteins,[5c] as well as in the modification of other supramolecular structures.[6] However, these efforts have traditionally been carried out in solution.

In recent years, SPs on surfaces have attracted substantial interest,[7] because the chemical and electronic structures can be resolved at atomic precision using scanning tunneling microscopy (STM), providing critical insights into properties and functions of SPs. Pre-functionalization of SPs has been extensively used to prepare one-dimensional SPs on surfaces with superb structural, chemical, and functional tunability. This pre-functionalization involves varying the functional groups on precursors (*e.g.* carboxylic acid, pyridyl, cyano and hydroxyl end groups) or their geometries (*e.g.* linear rod-like, tripod star-like, kinked and bent).[8] However, on-surface pre-functionalization is incompatible with precursors that contain highly reactive functional groups, such as alkenyl and isocyano groups, because they do not withstand the annealing process of evaporation onto a substrate.

An alternative is on-surface post-functionalization, but this has not yet been used due to lack of suitable on-surface reactions. Taking advantage of our recent development of Heck cross-coupling and divergent cross-coupling reactions on surfaces,[9,10] we here report the on-surface post-functionalization of metal-coordinated SPs and self-assembled SPs, both deriving from the same precursor 5,10,15-tri-(4-pyridyl)-20-bromophenyl porphyrin (Br-TPyP). The metal-coordinated SPs were readily decorated at both edges through Heck reaction with 4-vinyl-1,1'-biphenyl (VBP) to afford functionalized metal-coordinated SPs (Figure 1a). However, the metal-coordinated SPs could not undergo divergent cross-coupling with 4-isocyano-1,1'-biphenyl (ICBP). The SPs decomposed because the coordination of the isocyano group with Cu was stronger than that of the pyridyl group with Cu. In the absence of Cu, the precursor Br-TPyP self-assembled into SPs possessing planar chirality, which induced divergent cross-coupling as an enantioselective reaction to afford homochiral functional units (Figure 1b).

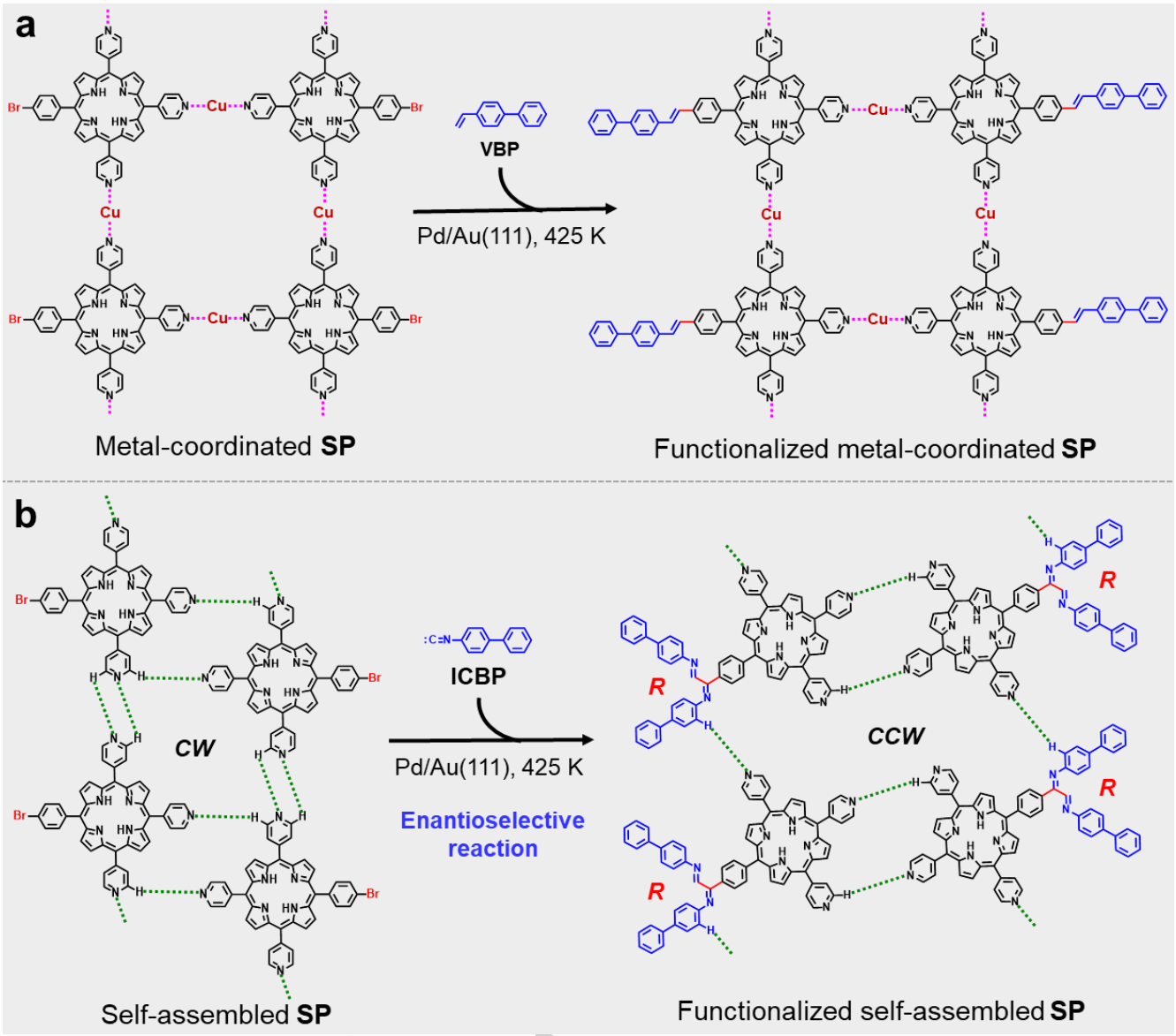

Figure 1. On-surface post-functionalization of metal-coordinated (a) and self-assembled (b) SPs via cross-coupling reactions. Pink dotted lines in Figure 1a indicate a pyridyl-Cu-pyridyl coordination bond. The green dotted lines in Figure1b indicate weak hydrogen bonding or van der Waals interactions.

Results and Discussion

Porphyrin frameworks offer a wide spectrum of physicochemical and photoelectric properties with diverse applications,[11] which make ideal platforms for constructing versatile supramolecular multiporphyrin architectures.[12] To develop on-surface post-functionalization, we selected Br-TPyP as the precursor. In Br-TPyP, three pyridyl groups can direct the formation of SPs through non-covalent interactions, and the single bromobenzene group can participate in on-surface cross-coupling after SP formation.[9,10] In addition, the porphyrin backbone of the SPs can promote and maintain adsorption onto the surface, preventing dispersion during post-functionalization.[13]

First, we tried to post-functionalize metal-coordinated SPs by conducting an on-surface Heck reaction with VBP (Figure 1a). A submonolayer of Br-TPyP molecules and Cu atoms (~0.1 ML) were successively deposited onto a pristine surface of Au(111) held at room temperature. After annealing at 353 K for 15 min, the sample was cooled to 120 K and analyzed by STM, which revealed the desired ladder-shaped SPs, arising from the coordination of pyridyl groups in Br-TPyP with Cu (Figure 2a). The ladders aligned ~ ±8° from [$\bar{1}$10] or equivalent orientation on Au(111).[8j] The bromide moieties of the Br-TPyP were intact and exposed on both sides of the metal-coordinated SPs (Figure 2d), consistent with previous reports.[8k]

Next, excess VBP molecules followed by ~0.1 momolayer Pd atoms were dosed onto the surface of the Au(111) sample. Annealing to 425 K induced Heck reaction of bromides and alkene molecules to form functionalized SPs. Large-scale STM

images (Figure 2b) revealed that the functionalized SPs mantained an intact ladder-shaped structure, which predominantly aligned ~ ±8° from [$\bar{1}$10] or equivalent orientation, consistent with the alignment of the metal-coordinated SPs before functionalization. Most bromide moieties along the two edges of the ladder were occupied with rod-like structures (blue and pink dotted frames in Figure 2b), originating from alkene precursors. The porphyrin backbone was studded with rod-like structures extending outward perpendicularly (Figure 2e), which were generated through *trans*-Heck reaction. Rod-like structures parallel to the backbone were attributed to *cis*-Heck reaction (pink dotted frame in Figure 2f).[9] Moreover, statistical analysis showed that the abundance of post-functionalized products via Heck reaction with VBP was up to ~72% (Figure 2c), indicating that the metal-coordinated SPs could be efficiently post-functionalized by on-surface Heck reaction.

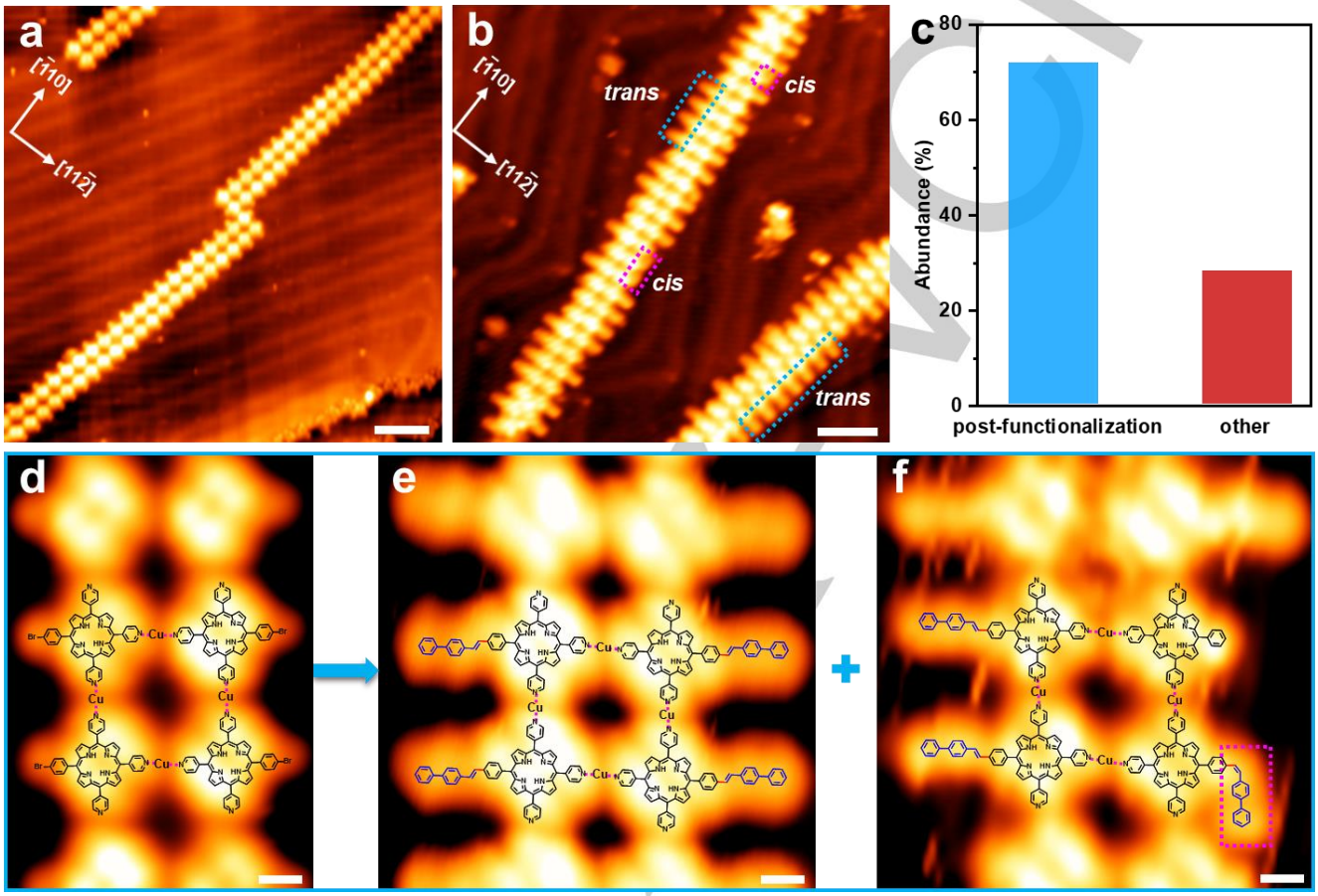

Figure 2. On-surface post-functionalization of metal-coordinated SPs with VBP on Au(111) in the presence of Pd. (a) STM image of metal-coordinated SPs before functionalization. (b) STM image of metal-coordinated SPs after functionalization. (c) Statistical abundance of post-functionalized products via the Heck reaction with VBP. (d) High-resolution STM image of an individual metal-coordinated SP. (e,f) High-resolution STM image of two individual functionalized SPs. Scale bars: (a,b) 5 nm. (d,e and f) 0.5 nm. Tunneling parameters: (a) U = -1.85 V, I = 0.07 nA. (b) U = -2.51 V, I = 0.07 nA. (d) U = -2.51 V, I = 0.09 nA. (e) U = -2.51 V, I = 0.1 nA. (f) U = -2.51 V, I = 0.07 nA.

To introduce different functional groups into SPs, we attempted to functionalize the metal-coordinated SPs with ICBP, in the hope of achieving on-surface divergent cross-coupling.[10] After preparing the metal-coordinated SPs on the Au(111) surface, excess molecules of ICBP followed by ~0.1 monolayer Pd atoms were dosed onto the surface at room temperature, and the sample was annealed at 425 K for 30 min. Surprisingly, the metal-coordinated SPs completely decomposed (Figure 3a), resulting in numerous discrete oligomers with a bright core surrounded by multiple rod-like branches. The bright cores consisted of one or several saddle-shaped structures,[8j] which can be attributed to self-assembly of porphyrins from Br-TPyP via hydrogen bonding or van der Waals interactions.[14] STM images of representative oligomers showed that the branches included V-shaped structures attached to the porphyrin (white dotted circles in Figure 3b, 3c, 3e and 3f) and rod-like structures without obvious connection to porphyrin. One V-shaped structure in the STM images can be attributed to the product of the divergent cross-coupling reaction involving one Br-TPyP and two ICBP molecules,[10] and the rod-like structures can be considered to be intact ICBP molecules attached to the porphyrin via a two-fold isocyano–Cu–pyridyl bond, three-fold (isocyano)$_2$–Cu–pyridyl bond or isocyano–Cu–imine bond. Consistent with this interpretation, none of these structures formed in the absence of exogenous Cu atoms. Moreover, we carried out density functional theory (DFT) calculation and STM simulation based on the proposed structures, which agreed with the corresponding experimental STM images (see Figure S1 in Supporting Information).

Statistical analysis of the saddle-shaped structure in the oligomer core revealed four major classes of oligomers (Figure 3d). The most abundant was monomer with a core consisting of one porphyrin, followed by dimer with a core of two porphyrins. The tetramer with a core of four porphyrins was more abundant than the trimer. Altogether these four oligomers accounted for approximately 93% of all observed oligomers. However, the abundance of divergent cross-coupling products was only 34% (see Figure S2 in Supporting Information), probably because of steric hindrance resulting from the pyridyl-Cu-ICBP coordination.

To clarify the driving force for the decomposition of metal-coordinated SPs, some control experiments were performed. When Pd but without ICBP was introduced onto the surface containing the Cu-coordinated SPs, the ladder-shaped structure is intact even after annealing to 425 K (see Figure S3 in Supporting Information). In contrast, depositing ICBP but without Pd led to the decomposition of ladder-shaped structure of SPs (see Figure S4 in Supporting Information). The results demonstrated that ICBP induced the decomposition of Cu-coordinated SPs, rather than Pd. Furthermore, DFT calculations showed that the reaction energy of pyridyl–Cu–isocyano coordination was 0.41 eV lower than that of pyridyl–Cu–pyridyl coordination (see Figure S5 in Supporting Information). Therefore, the conversion of pyridyl–Cu–pyridyl into pyridyl-Cu–isocyano is thermodynamically favorable, which would explain the observed disassembly of metal-coordinated SPs.

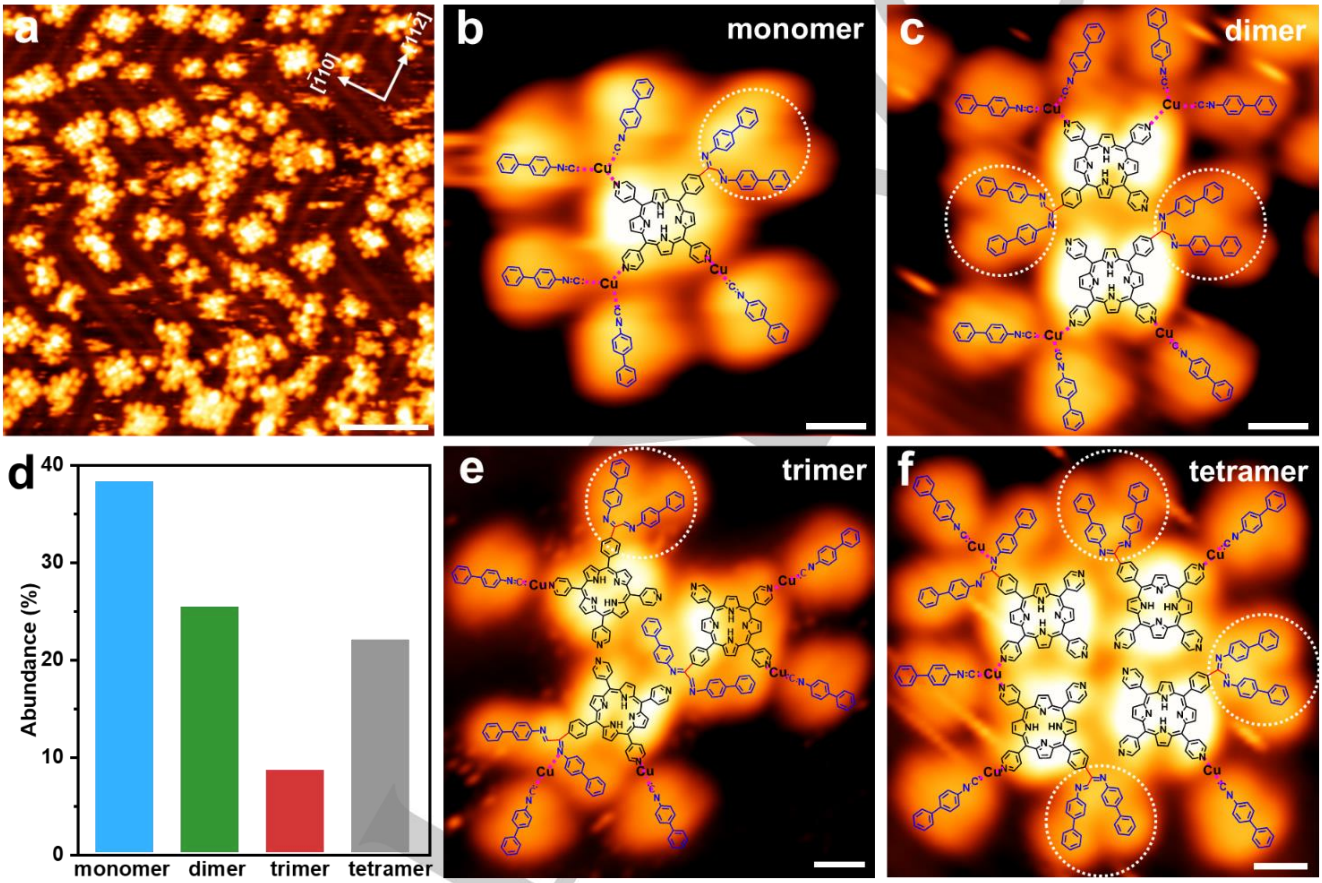

Figure 3. The reaction of metal-coordinated SPs with ICBP on Au(111) in the presence of Pd. (a) STM image of metal-coordinated SPs after the reaction with ICBP at 425 K. (b, c, e and f) Close-up STM images of four representative oligomers: monomer (b), consisting of one porphyrin moiety; dimer (c), consisting of two porphyrin moieties; trimer (e), consisting of three porphyrin moieties; tetramer (f), consisting of four porphyrin moieties. (d) Statistical abundance of four representative oligomers. Scale bars: (a) 10 nm. (b, c, e and f) 0.5 nm. Tunneling parameters: (a,f) U = -1.90 V, I = 0.08 nA. (b) U = -1.85 V, I = 0.09 nA. (c) U = -1.90 V, I = 0.07 nA. (e) U = -1.85 V, I = 0.14 nA.

To avoid interference of Cu in the divergent cross-coupling reaction, we tried to prepare SPs self-assembled by weaker interactions, such as hydrogen bonds or van der Waals interactions, in the absence of Cu. A submonolayer of Br-TPyP molecules was prepared via evaporation onto Au(111) substrate held at room temperature, and double-stranded SPs formed through self-assembly (Figure 4a). The SPs aligned at ~ ±15° along [11$\bar{2}$] or equivalent orientations on Au(111), and intact bromo-substituents were visible along both sides. Careful inspection revealed that the self-assembled SPs were chiral structures including two homochiral chains, a clockwise (*CW*) chiral SP and counterclockwise (*CCW*) chiral SP. The enantiomeric SPs from Br-TPyP were identified based on the arrangement of four adjacent porphyrin unit cells (Figure 4d and 4f), each measuring a = 1.46 ± 0.03 nm, b = 1.90 ± 0.03 nm, and θ = 120 ± 3°. High-resolution STM images of the chiral SPs showed that two Br-TPyP molecules staggered to form a dimer with planar chirality, and the type of staggering determined the chirality. A dimer unit was stabilized by lateral intermolecular C–H···N interactions along the short axis (black arrow in Figure 4d and 4f), and the dimer units arranged into a double strand via

vertical intermolecular interactions, such as hydrogen bonds or van der Waals interactions.[14]

After formation of the enantiomeric SPs on the Au(111) surface, excess ICBP molecules and Pd atoms (~0.1 ML) were deposited onto the surface at room temperature, which was then annealed at 425 K for 30 min. STM images showed the divergent cross-coupling reaction occurred and the functionalized SPs arranged along the [11 $\bar{2}$] or equivalent orientations. The porphyrin unit cell parameters were a' = 1.46 ± 0.03 nm, b' = 1.67 ± 0.03 nm, and θ' = 84 ± 3° (Figure 4e and 4g). Two sides of the functionalized SPs showed V-shaped branches originating from two ICBP precursors. Functionalized products resulting from divergent cross-coupling of Br-TPyP with two ICBPs accounted for up to 85% of observed products (Figure 4c), demonstrating that this coupling allows efficient post-functionalization of self-assembled SPs.

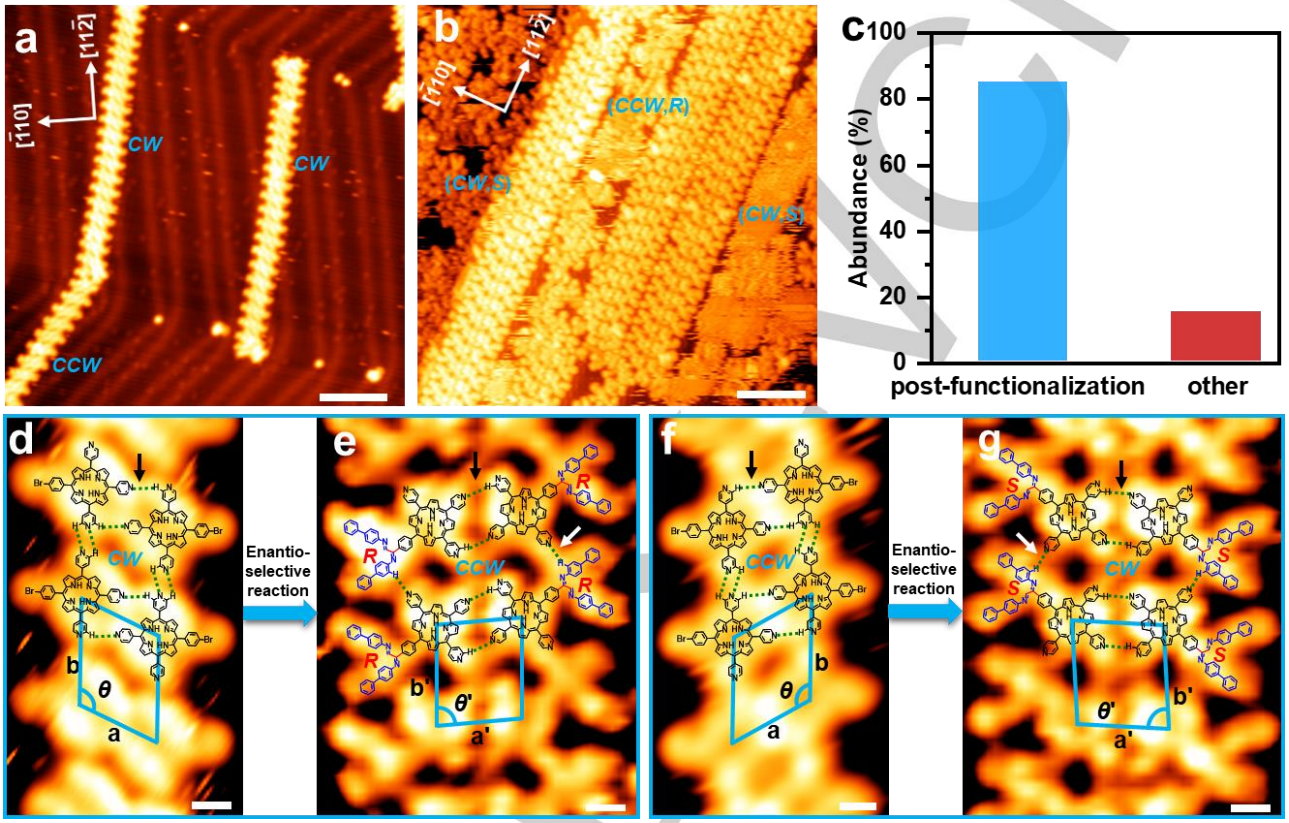

Figure 4. On-surface post-functionalization of self-assembled SPs via divergent cross-coupling reaction with ICBP on Au(111) in the presence of Pd. (a) STM image of self-assembled SPs derived from Br-TPyP. (b) STM image of self-assembled SPs after functionalization. (c) Statistical abundance of post-functionalized products via the divergent cross-coupling reaction with ICBP. (d,f) High-resolution STM images of individual *CW*-SP (d) and *CCW*-SP (f). (e,g) High-resolution STM images of individual functionalized (*CCW*,*R*)-SP (e) and individual functionalized (*CW*,*S*)-SP (g). Scale bars: (a,b) 5 nm, (d-g) 0.5 nm. Tunneling parameters: (a) U = -2.51 V, I = 0.11 nA. (b,e,g) U = -1.40 V, I = 0.15 nA. (d) U = -2.51 V, I = 0.1 nA. (f) U = -2.51 V, I = 0.09 nA.

Image analysis of the functionalized products from the preformed chiral SPs demonstrated that the planar chirality of the two unfunctionalized enantiomers, chiral *CW*-SP and chiral *CCW*-SP, inverted after the divergent cross-coupling reaction, due to rotation of the monomers (Fig. 4d-4g). Much more important, all the chiral *CCW*-SP backbones had attached with *R*-enantiomers on both edges to afford (*CCW*,*R*)-SP products (Figure 4e), with no *S*-enantiomers observed in the chains. Moreover, in the enantiomeric product (*CW*,*S*)-SPs, only *S*-enantiomers were observed on both edges (Figure 4g). These surprising results indicated that the chiral-assembly of SPs might induce enantioselective divergent cross-coupling reaction.

Another post-assembly pathway was possible: first the preformed SPs decomposed, then the resulting monomers underwent nonselective divergent cross-coupling reaction with ICBP to generate (*R*)- and (*S*)-monomer products. Finally, the two enantiomers selectively self-assembled into functionalized (*CCW*,*R*)- and (*CW*,*S*)-SPs. For the self-assembly of the (*R*)- and (*S*)-monomer product, 16 possible homochiral dimer structures were envisaged, all stabilized by weak interactions involving pyridyl groups, such as hydrogen bonding or van der Waals interactions (see Figure S6 and S7 in Supporting Information). Due to symmetry matching, only the following four dimers should self-assemble into double-strand SPs: (*CCW*,*R*)-SP, (*CW*,*R*)-SP, (*CW*,*S*)-SP and (*CCW*,*S*)-SP (see Figure S8 in Supporting Information). DFT calculations predicted that the diastereoisomers (*CCW*,*R*)-SP and (*CW*,*R*)-SP could self-assemble from (*R*)-monomer product, and that their total energies were very similar to each other, with a difference of only 0.24 eV between the energies of the two unit cells (see Figure S9 in Supporting Information).

During experiments, only (*CCW*,*R*)-SPs and (*CW*,*S*)-SPs were observed but not (*CCW*,*S*)-SPs or (*CW*,*R*)-SPs. These results argue against a post-assembly pathway involving SP decomposition followed by nonselective divergent cross-coupling. Instead, the experimental results favor an enantioselective reaction pathway induced by chiral assembly.

To clarify the driving force responsible for the enantioselective transformation of preformed chiral SPs into functionalized SPs, we conducted DFT calculations to compare the energies of the intermediate **A** after the first addition of ICBP and the intermediate **A'** after rotation of ~30° (Figure 5), according to the mechanism of divergent cross-coupling reaction.[10] The calculations predicted that the intermediate **A'** was more stable than the intermediate **A**, and that the stabilization energy of each unit cell was 0.37 eV (see Figure S10 in Supporting Information), indicating the rotation of intermediate **A** to form intermediate **A'** is the thermodynamically favorable pathway. In particular, in the second addition of ICBP to the intermediate **A'**, the direction of attack leading to the *S*-enantiomer (red solid arrow in Figure 5) is prohibited due to steric hindrance, resulting in only formation of the *R*-enantiomer (green solid arrow in Figure 5). This would explain the enantioselectivity of the divergent cross-coupling reaction of Br-TPyP with two ICBPs and the planar chirality of SPs is crucial to induce the enantioselectivity. It is noteworthy that this chiral assembly-induced divergent cross-coupling reaction itself is enantioselective, rather than the transfer of the chiral arrangement from the assembled molecules to covalently connected products in previous reports.[15]

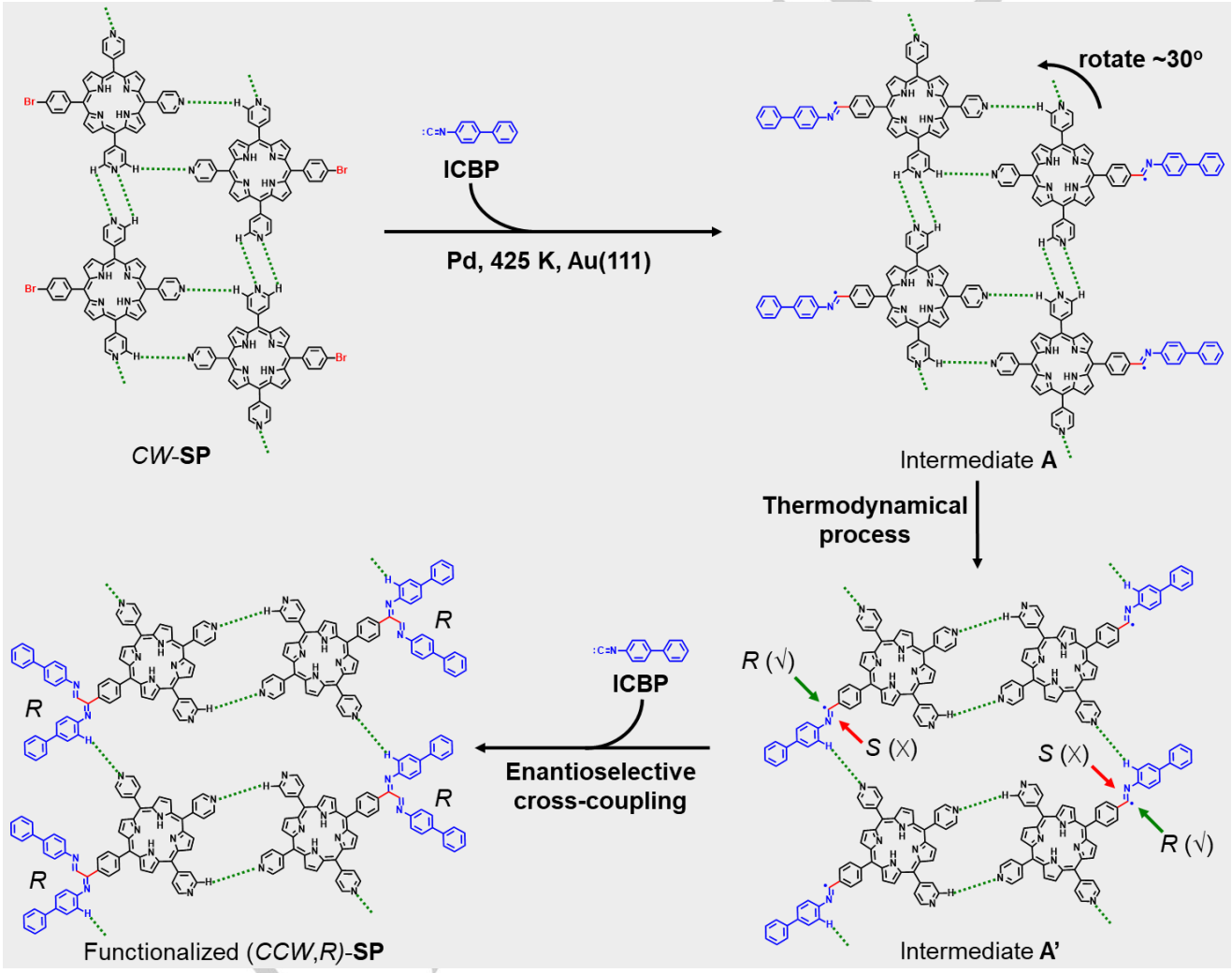

Figure 5. Proposed reaction pathway for post-functionalization of chiral SPs via enantioselective cross-coupling reaction with ICBP.

Conclusion

We have developed the first on-surface post-functionalization of metal-coordinated or self-assembled SPs derived from the same precursor Br-TPyP. Ladder-shaped, metal-coordinated SPs undergo on-surface Heck reaction with VBP to form functionalized SPs with excellent selectivity of cross-coupling, without obvious formation of homo-coupling products. However, the on-surface reaction of Br-TPyP with ICBP leads to the depolymerization of the metal-coordinated SPs to form porphyrin oligomers surrounded by coordinated ICBP molecules, because of the stronger coordination ability of ICBP with Cu in comparison with Br-TPyP. In the absence of Cu, the precursor

Br-TPyP forms chiral SPs via self-assembly, which readily undergo on-surface enantioselective divergent cross-coupling with ICBP to afford functionalized homochiral SPs. DFT calculations suggest that the enantioselectivity originates from the chirality of self-assembly in the preformed SPs. The key to achieve the post-functionalization of SPs is the suitable cross-coupling reaction with high reactivity and selectivity. Moreover, the careful selection of SPs and reactants in the post-functionalization is essential to avoid their incompatibility. Our protocol of post-functionalization on surfaces would provide the possibility to broaden concept of on-surface chemistry in constructing novel molecular nano-structures, and the striking discovery that chiral self-assembly can lead to enantioselective reaction may help guide the challenging exploration of on-surface enantioselective reactions.

Acknowledgements

This work was supported by the National Natural Science Foundation of China (Nos. 21925201 and 91845110), Shanghai Municipal Science and Technology Major Project (Grant No. 2018SHZDZX03), Natural Science Foundation of Shanghai (20ZR1414200), the Programme of Introducing Talents of Discipline to Universities (B16017), Program of the Shanghai Committee of Sci. & Tech. (Project No. 18520760700) and the Program for Eastern Scholar Distinguished Professor. We thank the Research Center of Analysis and Test of East China University of Science and Technology for help in the characterization.

Keywords: on-surface reactions • post-functionalization • supramolecular polymers • enantioselective reaction • scanning tunneling microscopy

[1] T. F. A. de Greef, E. W. Meijer, *Nature* **2008**, *453*, 171–173.

[2] T. Aida, E. W. Meijer, S. I. Stupp, *Science* **2012**, *335*, 813–817.

[3] a) L. Brunsveld, B. J. B. Folmer, E. W. Meijer, R. P. Sijbesma, *Chem. Rev.* **2001**, *101*, 4071–4097; b) G. R. Whittell, M. D. Hager, U. S. Schubert, I. Manners, *Nat. Mater.* **2011**, *10*, 176−188; c) L. Yang, X. Tan, Z. Wang, X. Zhang, *Chem. Rev.* **2015**, *115*, 7196−7239; d) E. Krieg, M. M. C. Bastings, P. Besenius, B. Rybtchinski, *Chem. Rev.* **2016**, *116*, 2414–2477.

[4] M. Weck, *Polym. Int.* **2007**, *56*, 453–460.

[5] a) M. S. T. Goncalves, *Chem. Rev.* **2009**, *109*, 190–212; b) J. Schoch, M. Wiessler, A. Jäschke, *J. Am. Chem. Soc.* **2010**, *132*, 8846–8847; c) S. Khan, S. Sur, P. Y. W. Dankers, R. M. P. da Silva, J. Boekhoven, T. A. Poor, S. I. Stupp, *Bioconjugate Chem.* **2014**, *25*, 707−717.

[6] a) M.-M. Gan, J.-Q. Liu, L. Zhang, Y.-Y. Wang, F. E. Hahn, Y.-F. Han, *Chem. Rev.* **2018**, *118*, 9587−9641; b) A. Proust, B. Matt, R. Villanneau, G. Guillemot, P. Gouzerh, G. Izzet, *Chem. Soc. Rev.* **2012**, *41*, 7605–7622; c) A. S. Goldmann, M. Glassner, A. J. Inglis, C. Barner-Kowollik, *Macromol. Rapid Commun.* **2013**, *34*, 810−849; d) H. Durmaz, A. Sanyal, G. Hizal, U. Tunca, *Polym. Chem.* **2012**, *3*, 825−835.

[7] a) T. Yokoyama, S. Yokoyama, T. Kamikado, Y. Okuno, S. Mashiko, *Nature* **2001**, *413*, 619–621; b) J. V. Barth, G. Constantini, K. Kern, *Nature* **2005**, *43*, 671–679; c) J. V. Barth, *Annu. Rev. Phys. Chem.* **2007**, *58*, 375–407; d) S. Stepanow, N. Lin, J. V. Barth, *J. Phys: Condens. Matter.* **2008**, *20*, 184002; e) N. Lin, S. Stepanow, M. Ruben, J. V. Barth, *Top. Curr. Chem.* **2009**, *287*, 1–44; f) R. Gutzler, S. Stepanow, D. Grumelli, M. Lingenfelder, K. Kern, *Acc. Chem. Res.* **2015**, *48*, 2132–2139; g) R. Mas-Ballesté, J. Gómez-Herrero, F. Zamora, *Chem. Soc. Rev.* **2010**, *39*, 4220–4233; h) M. Ouchi, N. Badi, J.-F. Lutz, M. Sawamoto, *Nat. Chem.* **2011**, *3*, 917–924; i) L. Dong, Z. Gao, N. Lin, *Prog. Surf. Sci.* **2016**, *91*, 101–135.

[8] a) A. Semenov, J. P. Spatz, M. Möller, J.-M. Lehn, B. Sell, D. Schubert, C. H. Weidl, U. S. Schubert, *Angew. Chem.* **1999**, *111*, 2701–2705; *Angew. Chem. Int. Ed* **1999**, *38*, 2547–2550; b) J. V. Barth, J. Weckesser, C. Cai, P. Günter, L. Bürgi, O. Jeandupeux, K. Kern, *Angew. Chem.* **2000**, *112*, 1285–1288; *Angew. Chem. Int. Ed.* **2000**, *39*, 1230–1234; c) A. Dmitriev, H. Spillmann, N. Lin, J. V. Barth, K. Kern, *Angew. Chem.* **2003**, *115*, 2774–2777; *Angew. Chem. Int. Ed.* **2003**, *41*, 2670–2673; d) T. Classen, G. Fratesi, G. Costantini, S. Fabris, F. L. Stadler, C. Kim, S. de Gironcoli, S. Baroni, K. Kern, *Angew. Chem.* **2005**, *117*, 6298–6301; *Angew. Chem. Int. Ed.* **2005**, *44*, 6142−6145; e) M. Surin, P. Samorì, A. Jouaiti, N. Kyritsakas, M. W. Hosseini, *Angew. Chem.* **2007**, *119*, 249–253; *Angew. Chem. Int. Ed.* **2007**, *46*, 245–249; f) S. L. Tait, A. Langner, N. Lin, S. Stepanow, C. Rajadurai, M. Ruben, K. Kern, *J. Phys. Chem. C* **2007**, *111*, 10982–10987; g) D. Heim, D. Écija, K. Seufert, W. Auwärter, C. Aurisicchio, C. Fabbro, D. Bonifazi, J. V. Barth, *J. Am. Chem. Soc.* **2010**, *132*, 6783–6790; h) M. Marschall, J. Reichert, A. Weber-Bargioni, K. Seufert, W. Auwärter, S. Klyatskaya, G. Zoppellaro, M. Ruben, J. V. Barth, *Nat. Chem.* **2010**, *2*, 131–137; i) W. Wang, Y. Hong, X. Shi, C. Minot, M. A. Van Hove, B. Z. Tang, N. Lin, *J. Phys. Chem. Lett.* **2010**, *1*, 2295–2298; j) Y. Li, J. Xiao, T. E. Shubina, M. Chen, Z. Shi, M. Schmid, H.-P. Steinrück, J. M. Gottfried, N. Lin, *J. Am. Chem. Soc.* **2012**, *134*, 6401−6408; k) J. Adisoejoso, Y. Li, J. Liu, P. N. Liu, N. Lin, *J. Am. Chem. Soc.* **2012**, *134*, 18526−18529; l) R. Shokri, M.-A. Lacour, T. Jarrosson, J.-P. Lère-Porte, F. Serein-Spirau, K. Miqueu, J.-M. Sotiropoulos, F. Vonau, D. Aubel, M. Cranney, G. Reiter, L. Simon, *J. Am. Chem. Soc.* **2013**, *135*, 5693−5698; m) M. Feng, H. Sun, J. Zhao, H. Petek, *ACS Nano* **2014**, *8*, 8644–8652; n) R. Zhang, G. Lyu, D. Y. Li, P. N. Liu, N. Lin, *Chem. Commun*. **2017**, *53*, 1731−1734; o) C. Krull, M. Castelli, P. Hapala, D. Kumar, A. Tadich, M. Capsoni, M. T. Edmonds, J. Hellerstedt, S. A. Burke, P. Jelinek, A. Schiffrin, *Nat. Commun.* **2018**, *9*, 3211.

[9] K.-J. Shi, C.-H. Shu, C.-X. Wang, X.-Y. Wu, H. Tian, P.-N. Liu, *Org. Lett*. **2017**, *19*, 2801–2804.

[10] D.-Y. Li, S.-W. Li, Y.-L. Xie, X. Hua, Y.-T. Long, A. Wang, P.-N. Liu. *Nat. Commun.* **2019**, *10*, 2414.

[11] a) K. Kadish, K. Smith, R. Guilard, *Handbook of Porphyrin Science*; World Scientific Publishing Company, 2010; b) M. O. Senge, M. Fazekas, E. G. A. Notaras, W. J. Blau, M. Zawadzka, O. B. Locos, E. M. Ni Mhuircheartaigh, *Adv. Mater.* **2007**, *19*, 2737–2774; c) H. Huang, W. Song, J. Rieffel, J. F. Lovell, *Front. Phys.* **2015**, *3*, 23; d) G. McDermott, S. M. Prince, A. A. Freer, A. M. Hawthornthwaite-Lawless, M. Z. Papiz, R. J. Cogdell, N. W. Isaacs, *Nature* **1995**, *374*, 517–521; e) A. W. Roszak, T. D. Howard, J. Southall, A. T. Gardiner, C. J. Law, N. W. Isaacs, R. J. Cogdell, *Science* **2003**, *302*, 1969–1972; f) S. Niwa, L.-J. Yu, K. Takeda, Y. Hirano, T. Kawakami, Z.-Y. Wang-Otomo, K. Miki, *Nature* **2014**, *508*, 228–232; g) R. J. Cogdell, A. Gall, J. Köhler, *Q. Rev. Biophys.* **2006**, *39*, 227–324; h) V. Sundström, *Annu. Rev. Phys. Chem.* **2008**, *59*, 53–77.

[12] a) J. Wojaczyński, L. Latos-Grażyński, *Coord. Chem. Rev.* **2000**, *204*, 113–171; b) I. Beletskaya, V. S. Tyurin, A. Y. Tsivadze, R. Guilard, C. Stern, *Chem. Rev.* **2009**, *109*, 1659–1713; c) J. A. A. W. Elemans, R. van Hameren, R. J. M. Nolte, A. E. Rowan, *Adv. Mater.* **2006**, *18*, 1251–1266; d) S. Durot, J. Taesch, V. Heitz, *Chem. Rev.* **2014**, *114*, 8542–8578.

[13] a) W. Auwärter, D. Écija, F. Klappenberger, J. V. Barth, *Nat. Chem.* **2015**, *7*, 105-120; b) J. Otsuki, *Coord. Chem. Rev.* **2010**, *254*, 2311–2341; c) S. Mohnani, D. Bonifazi, *Coord. Chem. Rev.* **2010**, *254*, 2342–2362.

[14] a) F. Vidal, E. Delvigne, S. Stepanow, N. Lin, J. V. Barth, K. Kern, *J. Am. Chem. Soc*. **2005**, *127*, 10101−10106; b) C. Meier, U. Ziener, K. Landfester, P. Weihrich, *J. Phys. Chem. B* **2005**, *109*, 21015−21027.

[15] a) P. C. M. Grim, S. De Feyter, A. Gesquière, P. Vanoppen, M. Rücker, S. Valiyaveettil, G. Moessner, K. Müllen, F. C. De Schryver, *Angew. Chem.* **1997**, *109*, 2713–2715; *Angew. Chem. Int. Ed. Engl.* **1997**, *36*, 2601–2603; b) H. Zhang, Z. Gong, K. Sun, R. Duan, P. Ji, L. Li, C. Li, K. Müllen, L. Chi, *J. Am. Chem. Soc.* **2016**, *138*, 11743–11748; c) A. Mairena, C. Wäckerlin, M. Wienke, K. Grenader, A. Terfort, K.-H. Ernst,

J. Am. Chem. Soc. **2018**, *140*, 15186–15189; d) B. Yang, N. Cao, H. Ju, H. Lin, Y. Li, H. Ding, J. Ding, J. Zhang, C. Peng, H. Zhang, J. Zhu, Q. Li, L. Chi, *J. Am. Chem. Soc.* **2019**, *141*, 168–174; e) N. Merino-Díez, M. S. G. Mohammed, J. Castro-Esteban, L. Colazzo, A. Berdonces-Layunta, J. Lawrence, J. I. Pascual, D. G. de Oteyza, D. Peña, *Chem. Sci.* **2020**, *11*, 5441–5446; f) H. Chen, L. Tao, D. Wang, Z.-Y. Wu, J.-L. Zhang, S. Gao, W. Xiao, S. Du, K.-H Ernst, H.-J. Gao, *Angew. Chem.* **2020**, *132*, 17566–17569; *Angew. Chem. Int. Ed.* **2020**, *59*, 17413–17416.

10.1002/anie.202016395

Entry for the Table of Contents

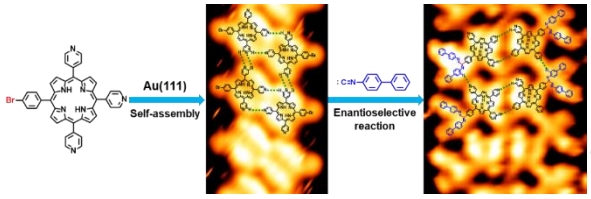

Post-functionalization on a surface: The first on-surface post-functionalization of two supramolecular polymers (SPs) derived from the same porphyrin precursor has been achieved via cross-coupling. Metal-coordinated SPs were easily decorated at both edges with 4-vinyl-1,1'-biphenyl via Heck reaction, while self-assembled chiral SPs underwent enantioselective cross-coupling with 4-isocyano-1,1'-biphenyl to acquire homochiral functional units.